Study on the Bearing Capacity of PVC Suction Caisson for Marine Aquaculture Cage under Monotonic Inclined Loading

Yukun Zhang[1,2,3], Pingsheng He[1,2], Dayong Li[1,2,3,*], Qian Xiang[1,2] and Boxian Li[1,2]

[1]*School of Civil Engineering and Architecture, Shandong University of Science and Technology, Qingdao 266590, China*

[2]*Shandong Key Laboratory of Marine Engineering Equipment Reliability and Intelligent Protection, Qingdao 266590, China*

[3]*Shandong Engineering Research Center of Marine Energy Geotechnical Engineering, China University of Petroleum (East China), Qingdao, 266580, China*

Abstract: As marine aquaculture cages are increasingly deployed in deeper waters, conventional foundation solutions are confronted with growing challenges associated with high installation and maintenance costs. This study proposes a corrosion-resistant, lightweight, high-strength, and low-cost PVC-made suction caisson for floating marine aquaculture cages in deep waters. A series of model tests were conducted to investigate the monotonic inclined bearing behavior of PVC suction caissons in sand, considering the influences of the aspect ratio and loading angle on the inclined bearing capacity and failure modes. The optimal loading angle is around 16° and the optimal suction caisson aspect is approximately 2.0, offering the highest bearing capacity at relatively small displacements. As the aspect ratio decreases or the loading angle increases, the motion behavior shifts from rotational failure to vertical pull-out failure. In addition, the PVC material exhibits a high safety margin in caisson wall strength around the loading point. Results also show that under the same inclined bearing capacity, the PVC suction caisson is the most cost-effective foundation type compared with the steel-made suction caisson and the gravity-base foundation. The application of PVC suction caissons in deep waters for marine aquaculture cages mooring systems exhibits sufficient reliability and promising prospects.

Keywords: PVC suction caisson, inclined pull-out capacity, motion behaviors, structural strength.

1. INTRODUCTION

Global marine aquaculture production reached 39.8 million tons accounting for 37.3% of total aquaculture production [1]. As marine aquaculture cages advance into deep waters, cage systems will face significantly enhanced environmental loads from wind, waves, and currents [1]. In deep waters, the control load of the mooring system is the inclined load. Traditional mooring systems primarily employ gravity-based foundations [3], pile foundations [4], and steel suction caissons [5] (Figure **1**). These types of foundation exhibit limitations in deep waters: gravity-based foundations rely on self-weight to provide bearing capacity; however, under deep waters conditions, the massive concrete blocks are difficult to transport and install. In addition, gravity-based foundations impose high requirements on seabed bearing capacity. In soft clay, gravity-based foundations tend to experience settlement and loss of stability. The steel pile foundations can provide high bearing capacity. However, they suffer from severe corrosion in marine environments [6]. Even with coatings and cathodic protection measures, steel pile foundations in harsh marine environments may lose 0.1–0.3 mm of cross-sectional thickness annually which are sufficient to undermine the bearing capacity of foundation structures within 10-20 years [7]. Protective coatings require regular maintenance and cathodic protection systems necessitate monitoring and anode replacement. These maintenance measures increase lifecycle costs, particularly in deep waters where implementation is extremely difficult.

Suction caissons are thin-walled cylindrical structures with a closed top and an open bottom, relying on the applied suction to achieve fast installation. Suction caissons have become one of the mature foundations in deep waters, particularly widely applied for fixing offshore wind turbines and platforms [8]. However, compared with offshore wind turbines, marine cage aquaculture has lower construction costs and requires lower requirements for foundation bearing capacity. The economic advantages of high-costs and high-load-bearing steel suction caissons in marine cage aquaculture are not obvious. Furthermore, the maintenance cost of the steel suction caisson is high, which further increases the continuous cost investment. Therefore, developing novel foundation materials that are lightweight, corrosion-resistant, easy to construct and cost-effective has become a critical technical problem urgently requiring resolution in marine aquaculture engineering.

Considering the lightweight and corrosion resistance of PVC, together with the high bearing capacity of suction caissons, this study proposes the

*Address correspondence to this author at the Shandong Engineering Research Center of Marine Energy Geotechnical Engineering, China University of Petroleum (East China), Qingdao, 266580, China;
E-mail: ldy@upc.edu.cn

Received on 05-08-2026 Accepted on 07-09-2026 Published on 09-09-2026

E-ISSN: 3083-3590/26

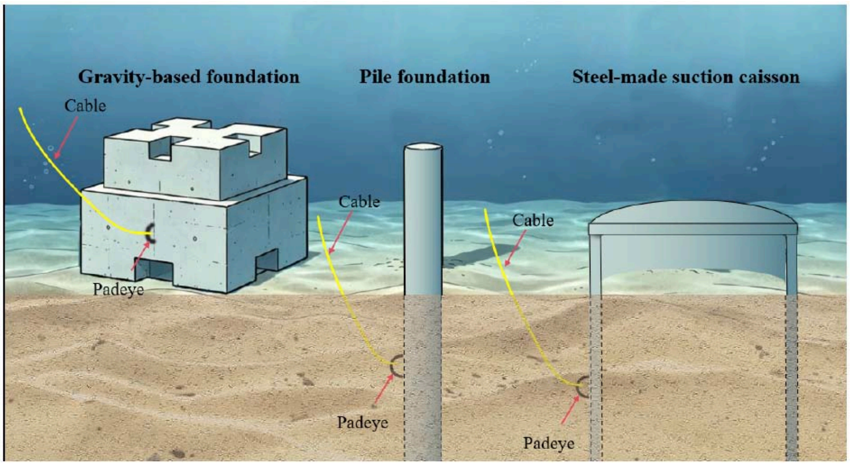

Figure 1: Diagrams of the gravity-based foundation, the pile foundation and the steel suction caisson.

PVC suction caisson as an innovative solution in deep waters. For mooring systems, the load at the padeye between the mooring chain and the caisson typically exhibits a significant inclination angle. In service conditions, suction caissons used for anchoring marine cages are subjected to inclined loads resulting from the combined action of waves and currents. Houlsby *et al*. [9] have established the yield envelope method for suction caissons under combined loading, laying the foundation for bearing capacity assessment under general loading conditions. Liang *et al*. [11] have investigated the bearing capacity of suction caissons under different inclined loading rates and loading depths through model tests. The suction under the lid plate rapidly increases as the loading rates change from 0.4 to 5 mm/s. Yang *et al*. [12] have studied the suction caissons bearing capacity in sand-over-clay by numerical simulation and proposed a calculation method for the inclined uplift bearing capacity of suction caissons at different soil layer positions. Cheng *et al*. [13] have employed a modified Mohr-Coulomb model to study the inclined uplift bearing capacity of suction caissons in calcareous sands, concluding that the padeye depth should be 0.6–0.7 times the foundation height and the loading angle should not exceed 30°. Bi [14] has determined that the angle between the mooring cable and the seabed should range between 8° and 24° through numerical simulation and theoretical derivation. Bai *et al*. [15] have investigated the motion patterns of skirted suction caissons under inclined loading through model tests and numerical simulation, establishing the relationship between the loading angle, padeye position, and the motion patterns of suction caissons.

PVC has been used in marine structures such as pile foundations and breakwater columns. [16]. Compared to steel, PVC has the characteristic of resistance to seawater corrosion, anti-biofouling, low cost, and ease of processing and molding [19]. In addition, PVC material is lighter than steel, which reduces the construction difficulty and transportation costs. Therefore, PVC materials have a promising application prospect in low-capacity marine environments. In marine engineering, PVC can serve as a material for structures such as marine pile foundations and breakwater columns [16]. Li *et al*. [20] have found that stress concentration in suction caissons occurs at the welding roots of the padeye and anchor walls by carrying out finite element simulation. In addition, stress magnitude is linearly influenced by padeye position, mooring load, and non-linearly affected by chain lift angle and the caisson deviation angle. Davies *et al*. [21] have discovered that PVC materials exhibit stable impact response and predictable energy absorption, demonstrating good flexibility through the drop hammer impact test.

Unlike conventional steel-made suction caissons, the application of PVC to suction caissons for aquaculture mooring systems remains largely unexplored in the literature. The PVC-made suction introduces fundamentally different design considerations: low stiffness, susceptibility to structural failure, and different interface friction characteristics that current design theories, primarily developed for steel caissons, cannot directly address. To address these limitations, this study aims to investigate the feasibility of using PVC suction caissons as mooring foundation for marine aquaculture cages. By applying monotonic loads, the bearing capacity, motion behaviors, and structural stability are examined. This work provides reference value for the application of PVC suction caissons in marine aquaculture cage systems.

2. MODEL TESTS SET-UP

2.1. Suction Caissons Models

Figure **2** gives the diagram of suction caisson model. The suction caisson models were made at a scale of

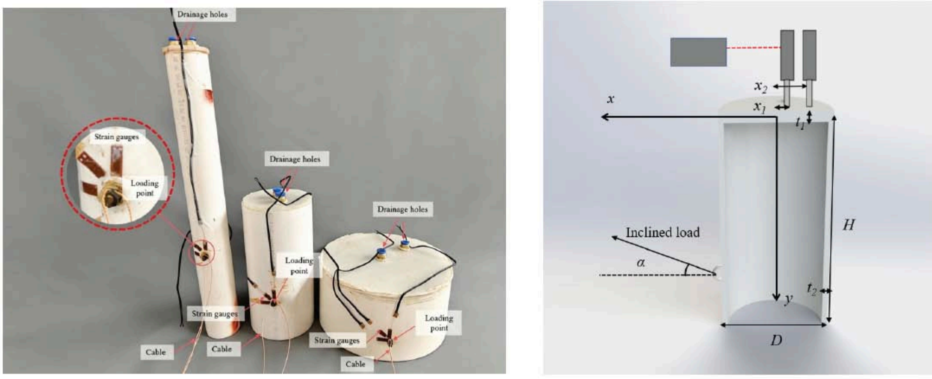

(a)Diagram of suction caisson models (b) Sketch of suction caisson model

Figure 2: Suction caisson models.

1:20 relative to the prototypes with identical sidewall material quantities and varying aspect ratios. The lid of each suction caisson features two drainage holes. During testing, the hole connected to the vacuum pump is sealed to achieve internal closure of the suction caisson. For all caisson models, the loading point is located at two-thirds [13] of the caisson height from the lid. Strain gauges are attached around the loading point at orientations of 0°, 45°, and 90° (showed in Figure **2a** to record strain during loading. Both the strain gauges and wiring are waterproofed to ensure they remain unaffected by water throughout the testing process. Tables **1** and **2** present the geometric and mechanical parameters of the suction caissons.

2.2. Test Apparatus

The schematic of the test apparatus is shown in Figure **3a**. The cylindrical steel soil tank of an inner diameter of 1.0 m and a height of 1.0 m is equipped with a drain valve at the bottom. The bottom of the tank is lined with a 10 cm layer of gravel and geotextile. The loading rig consists of a lateral servo actuator that provides monotonic inclined loads. The lateral servo actuator is equipped with a linear variable displacement transducer (LVDT) and a force transducer at the head of the rod. The force transducer is connected to a cable, which passes through a pulley and fixed to the loading point of the suction caisson. Since changes in the buoyancy of the float balls have minimal impact on the maximum cable tension, pulleys are used to replace the float balls [21]. Based on elastic similarity theory, a 0.9 mm nylon rope is used for the cable to accurately replicate the cable stress state. The loading angle can be adjusted by changing the height of the servo actuator and the position of the pulley. Two LVDTs are mounted on a guide rail via sliders, with the probes fixed to the suction caisson lid. When the suction caisson moves horizontally, the LVDTs will undergo corresponding horizontal displacement along the guide rail as the suction box moves. A laser displacement transducer is affixed to the guide rail to measure horizontal displacement of the LVDT. Thus, the three transducers can capture the motion behavior of the suction caisson.

2.3. Sand

The fine marine sand used in the tests was from Qingdao. The physical and mechanical parameters of the sand are presented in Table **3**. During sand preparation, the sand was uniformly deposited into the tank, maintaining the water level above the sand surface throughout the deposition process. To ensure repeatability, the sand within a depth of twice the caisson height was stirred and loosened before each

Table 1: The Suction Caisson Model Geometric Parameters

Height *H* (mm)	Outer diameter *D* (mm)	Aspect ratio	Wall thickness t_2 (mm)	Lid thinness t_1 (mm)	Weight *W* (N)
400	50	8.0	3		3.1
200	100	2.0	3	5	3.6
100	200	0.5	3		5.2

Table 2: The Suction Caisson Model Mechanical Parameters

Material	Elastic modulus *E* (GPa)	Poisson ratio *v*	Yield strength *σ* (MPa)	Density *ρ* (g/cm^3)
PVC	3.0	0.38	45	1.4

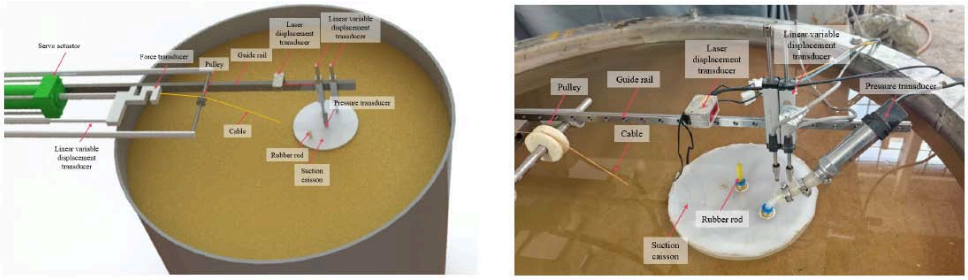

(a) Overview of test apparatus (b) Transducers layout

Figure 3: Test apparatus.

Table 3: The Physical and Mechanical Parameters of the Sand

Specific gravity of solids G_s	Angle of internal friction φ (°)	Coefficient of uniformity C_u	Coefficient of curvature C_c	Relative density D_r	Buoyant unit weight γ' (kN/m^3)	Saturated unit weight γ_{sat} (kN/mm^3)	Permeability coefficient k (mm/s)
2.65	24	1.18	0.965	0.96	9.98	19.78	0.002

test. Subsequently, water was added until the water level reached the top edge of the model box. Then the drainage valve was opened to lower the water level to 2 cm above the sand surface. This method was repeated twice to achieve a uniform degree of consolidation for the sand.

2.4. Test Procedure

Since the PVC density is only slightly higher than that of water, self-weight penetration cannot achieve internal seal state. In addition, the PVC suction caisson wall thickness is greater than that of a steel suction caisson. Therefore, the suction caissons were installed by jacking force and applied suction. The jacking force of 100 N was applied to the suction caisson lid. When the penetration depth no longer changed, the drainage hole was connected to the vacuum pump, and a pumping rate of 300 mL/min was maintained. Suction was stopped when sand particles appeared in the water extracted by the intelligent peristaltic vacuum pump, and penetration was considered complete. The soil plug height *p* of each suction caisson was measured and summarized in Table **4**.

Table **4** shows that as the aspect ratio increases, the soil plug height ratio to caisson height also increases. The reason is that to ensure the structural rigidity and strength of the PVC suction caisson, the wall thickness had to be increased (approximately 3–6 times that of a suction caisson of the same size). This causes the tip resistance to increase more rapidly with depth during the penetration. Moreover, the side friction increases quadratically with depth [10], both of which are unfavorable for the penetration of slender suction caissons. The tests were conducted under 1-g gravitational field conditions. The soil exhibited significant dilatancy, which led to a higher soil plug than that for the porotype suction caisson.

After penetration, the drainage hole was sealed. Then the caissons were left undisturbed in the sand substrate for a 1 h, allowing for full dissipation of excess pore pressure. To ensure repeatability, each test was performed at least three times. Table **4** also gives the loading parameters for the tests. The loading angle *α* is defined as the angle between the mooring line and the horizontal plane.

3. RESULTS AND DISCUSSIONS

3.1. Inclined Pull-Out Bearing Behavior

Kelly *et al*. [24] have established a dimensionless method to link small-scale test results with practical engineering data. All the test results in are presented in

Table 4: The Test Cases

Aspect ratio	Soil plug height *p* (mm)	Soil plug height ratio (%)	Loading angle *α* (°)	Monotonic loading rate (mm/s)
8.0	48	12.0	24	1.0
2.0	21	10.5	24	
			16	
			8	
0.5	10	10.0	24	

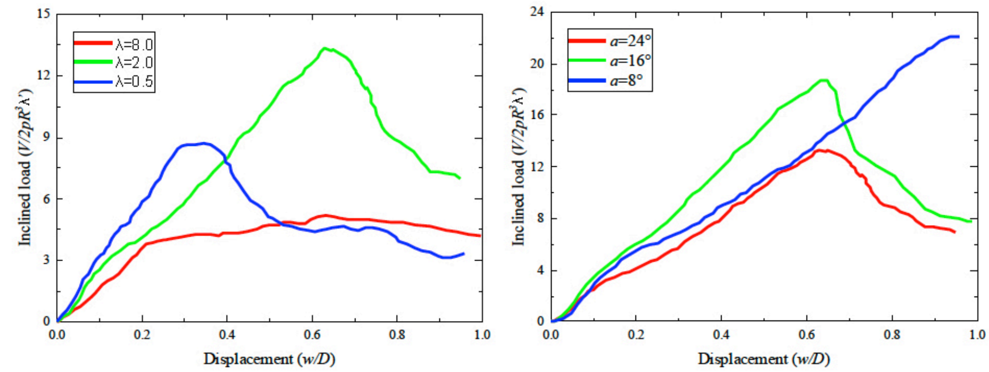

(a) Under various aspect ratios (*α*=24°) **(b) Under various loading angle (*λ*=2)**

Figure 4: Inclined load versus displacement curves.

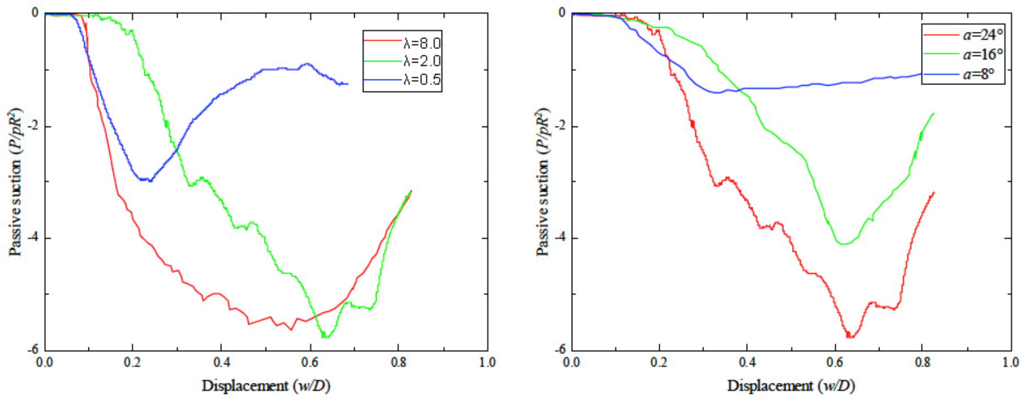

(a) Under various aspect ratios (*α*=24°) **(b) Under various loading angle (*λ*=2)**

Figure 5: Relationships between passive suction and displacement curves.

the normalized form. The displacement of loading point w is normalized as *w/D*, where *D* is the diameter of the suction caisson. The inclined load is normalized as $V/2\pi R^3\gamma'$, where *V* is the inclined load. *R* is the suction caisson radius. *γ'* is the soil buoyant unit weight. In addition, the passive suction is normalized as $P/\pi R^2$, where *P* is the peak passive suction. The dimensionless inclined load versus displacement curves for suction caissons with different aspect ratios under inclined loading are summarized in Figure **4**, and the dimensionless passive suction variation versus displacement curves are summarized in Figure **5**.

As shown in Figure **4a**, both the suction caisson inclined bearing capacity and the corresponding displacement decrease as the aspect ratio increases. In this study, the stage where the inclined load increases linearly with displacement is the initial loading stage. At the initial loading stage, the inclined load with the caisson aspect ratio of 0.5 increases fastest, while the one with the caisson aspect ratio of 8.0 increases slowly. Subsequently, the inclined load reaches a peak value. Then the inclined load either decreases or remains constant with increasing displacement. For suction caissons with aspect ratios of 2.0 and 0.5, the inclined load decreases after dimensionless displacements of 0.3 and 0.6, respectively, indicating possible local failure or sand softening. Whereas the inclined load of suction caisson with an aspect ratio of 8.0 exhibits no obvious peak value. The failure mode tends to be more progressive. This indicates that suction caissons with different aspect ratios have distinct failure modes, as discussed in Section 3.3.

According to Figure **4b**, for suction caissons with an aspect ratio of 2.0, a smaller loading angle corresponds to a higher pull-out bearing capacity. However, different loading angles do not linearly affect the inclined load growth rate with displacement: when *α*=16°, the growth rate is the highest; when *α*=8° and *α*=24°, the growth rate are the same and lower than that when *α*=16°. As a result, although the inclined pull-out bearing capacity is largest at a loading angle of 8°, the corresponding displacement is already close to one caisson diameter. This indicates that a smaller loading angle has a pronounced effect on bearing capacity at large displacements.

Figure **5** shows the passive suction variation versus displacement curves. Under monotonic inclined loading, passive suction was developed inside all suction

(a) Steel suction caisson (b) Gravity-based foundation models

Figure 6: Steel suction caisson and gravity-based foundation models.

Table 5: The Geometric Parameters of Steel Suction Caisson and Gravity-Based Foundation

Material	Outer diameter *D* (mm)	Side length (mm)	Aspect ratio	Wall thickness t_2 (mm)	Lid thinness t_1 (mm)	Weight W(N)
Steel	100	-	2.0	2	10	17.5
Concrete	-	200	1.0	-	-	196
	-	250	1.0	-	-	392

caissons. However, no passive suction was generated when the dimensionless loading point displacement is less than of 0.1 (Figure **5**). This is because at the initial stage of loading, the load displacement is mainly used to tension the cables. Under the circumstances, no relative displacement occurs between the sand and the caisson. Consequently, passive suction does not develop. Comparing Figures **4** and **5**, the inclined load and passive suction exhibit generally consistent trends, and two peak positions are close.

3.2. Bearing Capacities of Various Foundation Types

The bearing capacities of three foundation types (PVC suction caisson, steel suction caisson, and concrete gravity-based foundation) under monotonic inclined loading were investigated through model tests. Figure **6** shows the steel suction caisson and gravity-based foundation models. The geometric parameters are shown in Table **5**. The steel suction caisson aspect ratio is 2.0. Since the inclined bearing capacity is mainly provided by the passive earth pressure, the self-weight of the suction caisson has little impact on the bearing capacity. The gravity-based foundation models are 20 kg and 40 kg cubic concrete blocks.

Figure **7** shows the inclined load-displacement curves. The steel suction caisson has a wall thickness of 1.0 mm, with all other geometric dimensions identical to those of the PVC suction caisson.

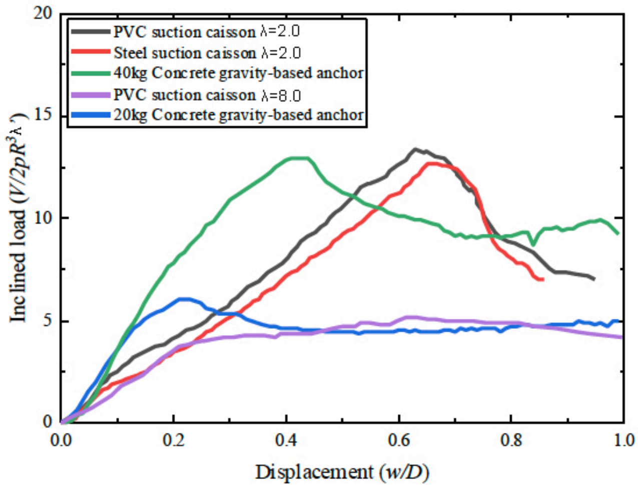

Figure 7: Inclined load-displacement curves for different material foundations.

Results show that all three foundation types exhibit typical elastoplastic load-displacement curves. At the initial loading stage, the inclined load increases approximately linearly with the loading point displacement, with the sand in an elastic compression state. When the load approaches the ultimate bearing capacity, the curve shows an obvious peak. The sand around the foundation then gradually enters a plastic failure stage, leading to an inclined load drop.

The steel and PVC suction caissons with an aspect ratio of 2.0 exhibit nearly identical inclined pull-out behavior. The steel suction caisson has a slightly lower inclined pull-out bearing capacity. The loading point displacement at the peak inclined load is slightly larger than that of the PVC suction caisson. This indicates that, within a certain material hardness range under inclined pull-out loading, the inclined load-displacement curve is not significantly affected. Due to its flexibility, the PVC material allows better development of passive earth pressure on the tension side sand, resulting in a slightly higher inclined pull-out bearing capacity than that of the steel suction caisson. Since this difference is not substantial, the design data of steel suction caissons can be referenced when designing PVC suction caissons.

The concrete gravity-based foundation provides inclined load through its self-weight and base friction. As seen in Figure **5**, the loading point displacement at the peak inclined load of the concrete gravity base is smaller than that of the suction caissons. As the loading point displacement increases, the concrete gravity base inclined load decreases and then stabilizes. The reduction magnitude is smaller than that of the suction caisson with an aspect ratio of 2.0. The 20 kg concrete gravity base has a slightly larger pull-out bearing capacity than the PVC suction caisson with an aspect ratio of 8.0; the 40 kg concrete gravity base has a slightly smaller inclined pull-out bearing capacity than the PVC suction caisson with an aspect ratio of 2.0.

Based on a 1:20 scale ratio, the cost comparison of the three prototype foundations made of different materials is summarized in Table **6**.

A direct comparison of the cost data shows that the economic performance of foundations varies significantly with material and structural type. The concrete gravity-based foundation has a very low material unit price, giving it a certain advantage in raw material cost. The gravity-based foundation only requires coating and crack repair. The maintenance cost only accounts for 1% of the construction cost. However, its self-weight is extremely large. This excessive weight greatly increases construction difficulty and imposes stringent demands on seabed bearing capacity, thus requiring additional soil treatment and reinforcement. Moreover, the construction process of a concrete gravity-based foundation involves multiple steps such as on-site casting, curing, and lowering, leading to a long construction period and high labor and machinery input. Under long-term seabed current scouring, the sand around the base is prone to erosion and hollowing, which significantly reduces the bearing capacity. Consequently, the structural stability and service safety are difficult to ensure in the long term.

The traditional steel suction caisson features high structural strength, convenient penetration construction, and excellent deformation inclined load. Nevertheless, its material unit price and total weight are both high, making the raw material cost far higher than those of the other two solutions. Steel is also susceptible to corrosion in the high-salt, high-humidity, and highly corrosive marine environment, requiring dedicated anti-corrosion coatings and regular maintenance measures. For the steel suction caisson, in addition to the annual visual inspection, a detailed underwater inspection is required every 5 to 10 years. This further increases the full-lifecycle operation and maintenance cost. For engineering applications with low bearing capacity requirements, such as marine aquaculture cages, the economic advantage of the steel suction caisson is difficult to realize.

In contrast, the PVC suction caisson demonstrates outstanding overall cost-effectiveness. Under the same dimensions, the raw material cost of a PVC suction caisson is only 10.8% of that of a steel suction caisson. Under equivalent bearing capacity conditions, its cost is 17.2%-29.7% of that of a concrete gravity base, showing a remarkable cost control advantage. The PVC suction caisson is the lightest in weight, yet it possesses excellent inclined pull-out bearing capacity. This fully demonstrates its significant advantages and practical value in engineering. Furthermore, the low density and light weight of PVC greatly reduce the difficulty and cost of transportation, lifting, further enhancing the overall economic benefit. In addition, PVC material has excellent corrosion resistance and only requires routine inspections; no additional corrosion prevention measures are necessary. Considering material cost, construction efficiency, maintenance difficulty, and marine environmental adaptability, the PVC suction caisson well balances

Table 6: Cost Comparison

Aspect ratio	Loading angle α (°)	Material	Unit Price (USD/ton)	Quality (tons)	Material Cost (thousand USD)	Installation Cost (thousand USD) [25]
2.0	24	PVC	750	2.94	2.2	4.4
2.0		Steel	500	40.80	20.4	60.7
-		Concrete	40	320	12.8	9.8
8.0		PVC	750	2.53	1.9	2.8
-		Concrete	40	160	6.4	4.9

structural bearing capacity and engineering economy. It is therefore a cost-effective foundation solution that meets the anchoring requirements of marine aquaculture cages.

3.3. Suction Caisson Motion Behavior during Loading

A coordinate system was established with the pre-loading midpoint of the suction caisson lid as the origin, as shown in Figure **1b**. This origin are fixed during the loading process. LVDTs were placed at positions x_1 and x_2, with corresponding vertical displacements v_1 and v_2. The laser displacement transducer measures the horizontal displacement (h) of the LVDTs. The vertical displacement of the suction caisson lid midpoint is calculated using Eq. (3). Because the caisson rotation angle was small, h was directly taken as the horizontal displacement of the origin.

$$\Delta x = \frac{v_2 x_1 - v_1 x_2}{x_1 - x_2} \tag{3}$$

$$\Delta y = h \tag{4}$$

The rotation angle was obtained using Eqs. (5)–(7).

$$\sin\theta = \frac{v_1 - v_2}{x_1 - x_2} \tag{5}$$

$$\cos\theta = \sqrt{1 - \sin\theta^2} \tag{6}$$

$$\theta = atant2(\sin\theta, \cos\theta) \tag{7}$$

The rotation center (x_c, y_c) can be obtained from Eqs. (8) and (9):

$$x_c = \frac{v_1 x_2 - v_2 x_1}{v_1 - v_2} \tag{8}$$

$$y_c = \frac{h(x_1 - x_2)}{v_1 - v_2} \tag{9}$$

The vertical and horizontal displacements of the lid midpoint are summarized in Figure **8**, and the rotation angle is summarized in Figure **9**.

As shown in Figures **8** and **9**, suction caissons with different aspect ratios exhibit different Motion behaviors under different loading angles. When the loading angle is 24°, the vertical displacement increases as the aspect ratio increases, while the horizontal displacement decreases. Among them, the suction caisson with an aspect ratio of 8.0 exhibits a predominantly vertical pull-out failure mode. The suction caisson with an aspect ratio of 2.0 exhibits a combined vertical pull-out and rotation failure mode. The suction caisson with an aspect ratio of 0.5 exhibits a predominantly rotation failure mode.

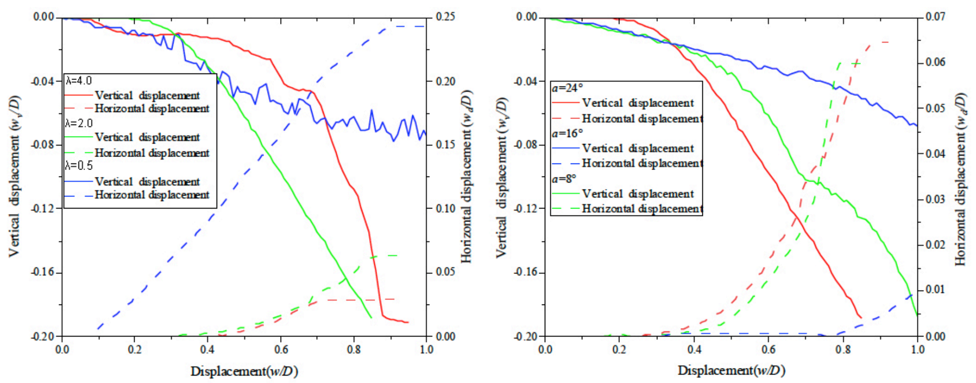

(a)Under various aspect ratios (α=24°) **(b) Under various loading angle (λ=2)**

Figure 8: Suction caisson lid midpoint displacement diagram.

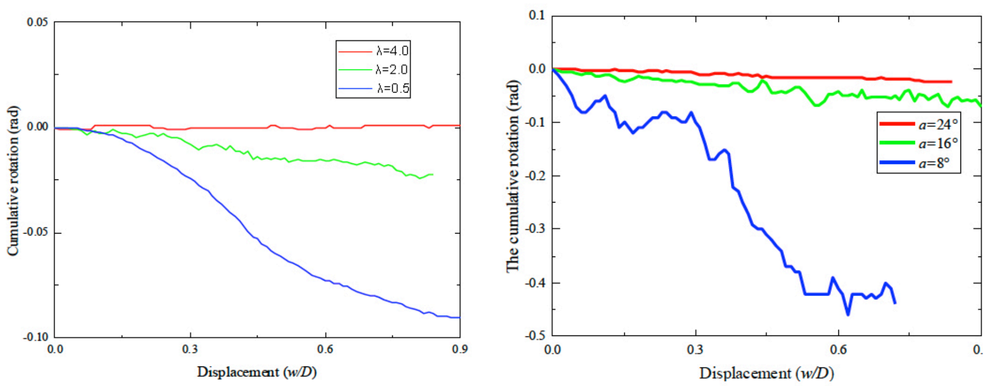

(a) Under various aspect ratios (α=24°) **(b) Under various loading angle (λ=2)**

Figure 9: Cumulative rotation angle diagram.

For a suction caisson with an aspect ratio of 2.0, a larger loading angle leads to larger vertical and horizontal displacements. At loading angles of 24° and 16°, the suction caisson exhibits a combined vertical pull-out and rotation failure mode. At a loading angle of 8°, it exhibits a predominantly rotation failure mode. The vertical displacement of the suction caisson generates significant passive suction, which explains why the passive suction is more pronounced at larger aspect ratios and larger loading angles in Figure **5**.

When the loading angle is 24°, the cumulative rotation of the suction caisson increases as the aspect ratio decreases. The caisson with an aspect ratio of 8.0 barely rotates. The caisson with an aspect ratio of 2.0 exhibits a small clockwise rotation. The caisson with an aspect ratio of 0.5 exhibits a clockwise rotation of 0.09 rad. This is because a suction caisson with a larger aspect ratio has a greater embedment depth, where the passive earth pressure is stronger. Consequently, the caisson cannot easily rotate, and its motion is dominated by vertical pull-out. In this case, the side friction and passive suction determine the upper limit of the suction caisson pull-out bearing capacity.

For a suction caisson with an aspect ratio of 2.0, the cumulative rotation decreases as the loading angle decreases. When the loading angle decreases from 24° to 8°, the cumulative rotation increases from 0.009 rad to 0.460 rad. When the loading angle becomes smaller, the vertical uplift force decreases, and the horizontal force increases. The failure mode then changes from vertical pull-out to rotation. Although a larger loading angle can save mooring line and space costs, it induces a larger vertical uplift force. Because the friction coefficient between PVC material and the sand is lower than that between steel and the sand, the PVC suction caisson cause a greater vertical displacement compared to the steel suction caisson. In this case, the horizontal passive earth pressure is not fully mobilized. Therefore, the suction caisson bearing capacity can be increased by appropriately reducing the loading angle.

The changes of the rotation center position with the loading point displacement are summarized in Figure **10**.

When the rotation center lies inside the suction caisson, the motion behavior can be considered rotation-dominated. When the rotation center lies outside the suction caisson, the motion behavior can be considered a combination of rotation and translation. When the rotation center is infinitely far away from the suction caisson, the motion behavior is pure translation.

Except for the suction caisson with an aspect ratio of 0.5, all suction caissons rotation center heights are near the lid height. As the loading point displacement increases, the rotation center gradually moves in the negative x-axis direction. Thus, these suction caissons initially undergo rotation-dominated motion. With increasing loading point displacement, they gradually change to a combined rotation-translation mode and eventually to pure vertical translation.

For the suction caisson with an aspect ratio of 0.5, the rotation center lies inside the caisson when the loading point displacement is less than 0.3. As the displacement increases, the rotation center continuously moves upward, eventually resulting in a combination of rotation and horizontal translation.

In Figures **10a**, **b**, and **c**, the calculated rotation centers within the range are relatively few, and the corresponding displacements are all less than 0.5. This is because when the suction caisson undergoes pure translation, the rotation center theoretically lies at infinity and cannot be shown in figures. Combined with Figures **10d** and **e**, it can be seen that a suction caisson exhibiting rotation failure has more identifiable rotation center points than one exhibiting vertical pull-out failure.

Based on the above research, the optimal loading angle is around 16° and the optimal suction caisson aspect is approximately 2.0. the determination of the optimal aspect ratio and loading angle is based on four parameters including the bearing capacity, the displacement corresponding to the bearing capacity, motion behavior and installation. The bearing capacity is evaluated using the peak inclined pull-out resistance as the primary indicator of ultimate limit state performance. In addition, the displacement corresponding to the inclined uplift bearing capacity should not be excessive, as excessive displacement will cause the cage to deviate from its predetermined position. The motion behavior is assessed based on the caisson movement mode, with vertical pull-out failure considered less favorable than rotation failure. Installation is another important consideration. The aspect ratio of 0.5 may compromise the internal sealing of the suction caisson, whereas the aspect ratio of 8.0 increases side friction makes installation more difficult.

3.4. Sand Deformation around Suction Caissons

Figure **11** shows the post-loading sand deformation around PVC suction caissons with different aspect ratios.

The sand deformation around the suction caisson is significantly influenced by the aspect ratio. The suction

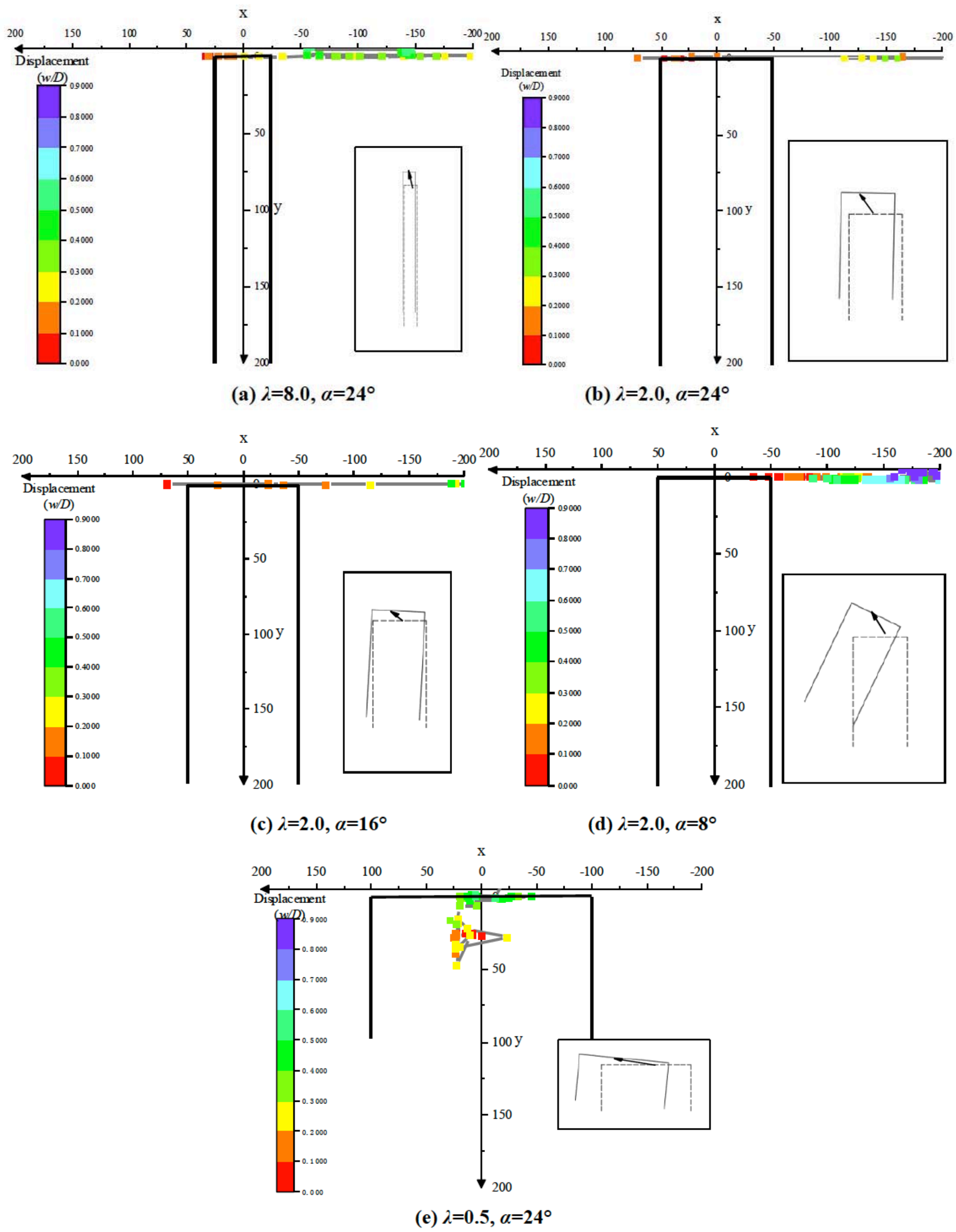

Figure 10: The rotation center position variation.

caisson with an aspect ratio of 8.0 exhibits vertical pull-out behavior, with negligible horizontal displacement and rotation. Consequently, its surrounding sand deformation pattern is completely different from that of suction caissons with aspect ratios of 2.0 and 0.5. Although Figure **11a** shows some heave on the front side relative to the rear side, the heave boundary is unclear and barely distinguishable by the naked eye, and the heave height is small. Therefore, the suction caisson with an aspect ratio of 8.0 has a minor effect on the surrounding sand. By contrast, suction caissons with aspect ratios of 2.0 and 0.5 both exhibit sand heave on the front side and sand settlement on the rear side. The heave zone is larger than the settlement zone. For the suction caisson with an aspect ratio of 2.0, the heave zone extends up to 2.5 times the caisson diameter, and the settlement zone extends up to about 1.3 times the caisson diameter. Both zones are nearly circular. For the suction caisson with an aspect ratio of 0.5, both the heave zone and the settlement zone are elliptical. The heave zone has a major axis up to 2 times the caisson diameter and a minor axis up to 1.3 times the diameter. The settlement zone has a major axis up to 1.3 times the caisson diameter and a minor axis about 1 time the diameter.

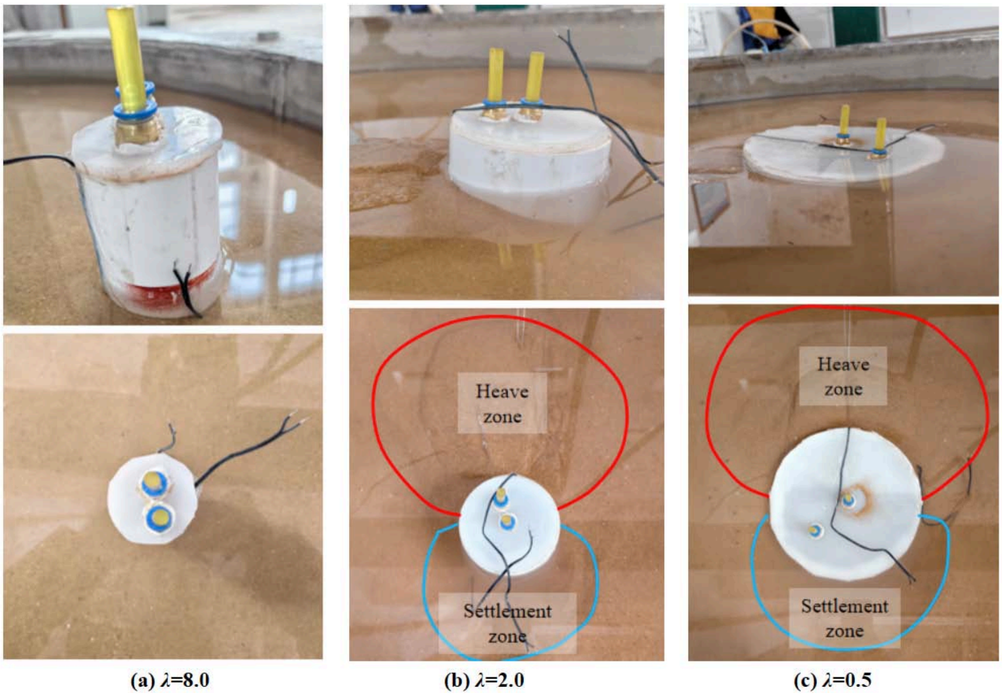

Figure 11: Sand deformation around the suction caisson.

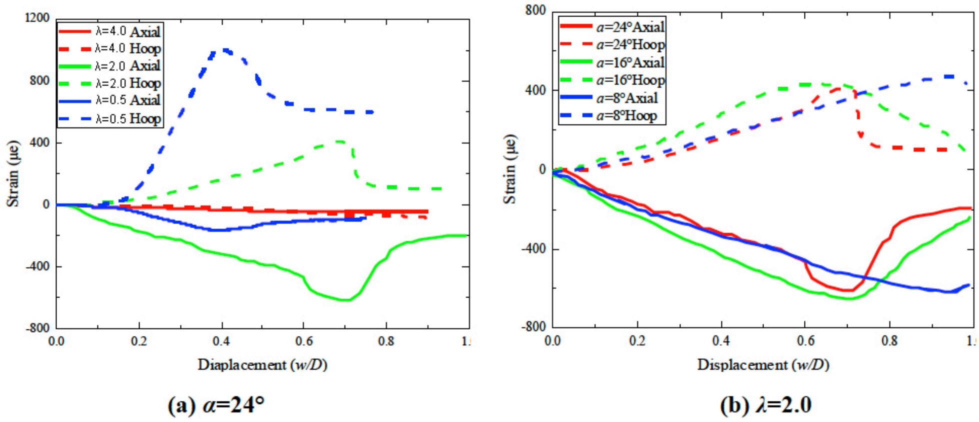

Figure 12: Strain around loading points.

3.5. Strain at Loading Point

The strength of PVC is lower than that of steel. Under loading, the caisson wall strain at the loading point may experience stress concentration, leading to structural failure. Therefore, for a PVC suction caisson, sand failure and structural failure must be considered. Figure **12** shows the axial and hoop caisson wall strain at the loading point.

Tensile hoop strain and compressive axial strain are developed at the loading point. Since the 45° strain value lies between the axial strain value and the hoop strain value, it has no impact on the stress calculation, the 45° strain value is no longer displayed. From Figure **12**, at a loading angle of 24°, the maximum strain increases as the aspect ratio decreases. The caisson with an aspect ratio of 8.0 exhibits the smallest strain. For the caisson with an aspect ratio of 2.0, the loading point strain reaches 600 με, with the axial strain larger than the hoop strain. For the caisson with an aspect ratio of 8.0, the loading point strain reaches 1000 με, with the hoop strain larger than the axial strain. This is because, for a thin-walled cylinder, the ability to resist local axial force depends mainly on its curvature and wall thickness. A smaller diameter gives a larger curvature and thus a stronger inclined load to flattening. For a cylinder with a larger diameter, the curved wall is flatter, making it more prone to local indentation and bending under external force, leading to a sharp increase in stress and strain in that region. Therefore, if the suction caisson stiffness is insufficient, the caisson stiffness can be increased by increasing the aspect ratio as long as the bearing capacity requirement is still met.

Figure **12b** shows the loading point strain under different loading angles. Comparing Figures **12b**

Table 7: The Verification Results of Various Aspect Ratio and Loading Angle

Aspect ratio	Loading angle *α*(°)	σ_1-σ_3 (MPa)	Yield strength *σ*(MPa)	Safety factor
8.0	24	0.284	45	158.5
2.0	24	2.256		19.9
	16	2.407		18.7
	8	2.408		18.7
0.5	24	3.575		12.6

and **4b**, the peak inclined load of the suction caisson occurs at the same loading point displacement as the peak strain. Moreover, the order of the peak strain magnitudes is consistent with the order of the pull-out bearing capacities of the corresponding caissons.

For the isotropic material, the generalized Hooke's law under plane stress conditions is:

$$\sigma_x = \frac{E}{1-\upsilon^2}(\varepsilon_x + \upsilon\varepsilon_y) \quad (10)$$

$$\sigma_y = \frac{E}{1-\upsilon^2}(\varepsilon_y + \upsilon\varepsilon_x) \quad (11)$$

$$\tau_{xy} = \frac{E}{2(1+\upsilon)}\gamma_{xy} = \frac{E}{2(1+\upsilon)}(2\varepsilon_{xy} - \varepsilon_x - \varepsilon_y) \quad (12)$$

where σ_x is the hoop stress; σ_y is the axial stress; τ_{xy} is the shear stress; ε_x is the hoop strain; ε_y is the axial strain; ε_{xy} is the 45° strain; γ_{xy} is the shear strain.

The Tresca strength theory was used for verification:

$$\sigma_{1,3} = \frac{\sigma_x+\sigma_y}{2} \pm \sqrt{(\frac{\sigma_x-\sigma_y}{2})^2 + \tau_{xy}^2} \quad (13)$$

where σ_1 and σ_3 are the maximum and minimum principal stresses, respectively. Under the plane stress assumption for a thin-walled cylinder, the radial stress is generally considered zero, so the intermediate principal stress σ_2 is assumed to be zero.

The loading point stress verification results are summarized in Table **7**.

As shown in Table **7**, the safety factor of the PVC material in the model tests exceeds 12 in all cases, indicating that the structural strength is fully sufficient to reach the sand failure limit. This also suggests that the wall thickness of the PVC suction caisson designed in this study is overly conservative. Subsequent tests will be conducted with thinner wall thicknesses to explore the balance among caisson cost, structural strength, and sand strength.

4. CONCLUSION

This study investigates the monotonic inclined pull-out bearing behavior of PVC suction caissons in sand under different aspect ratios and loading angles. The bearing capacity, motion behavior, and structural strain of the caissons were analyzed. The main conclusions are as follows:

(1) The inclined bearing capacity and motion behavior are governed by aspect ratio (λ) and loading angle (α). Capacity increases with α and is highest for λ=2.0. Decreasing λ or α shifts motion behavior from vertical pull-out to rotation, reducing passive suction. The passive suction is directly related to the vertical displacement of the caisson.

(2) The caisson wall structural safety factor of the PVC suction caissons in the model tests exceeds 12 in all conditions, which are sufficient to be used as foundations for marine cages. The loading point strain increases as the aspect ratio decreases, and a thin-walled cylinder with a larger diameter tends to develop higher stress.

(3) Under this study conditions, considering bearing capacity, displacement control, and structural safety together, λ=2.0 and α=16° are recommended to balance capacity and displacement control. Furthermore, subsequent research can improve the penetration effect by optimizing the wall thickness and further explore the sand bearing potential of PVC suction caissons.

(4) PVC suction caissons have a significant cost advantage, costing only 10.5%–39.7% of steel suction caisson or concrete foundations for comparable capacity. Considering construction efficiency, maintenance difficulty, and marine environmental adaptability, the economic advantage of the PVC suction caisson becomes even more prominent.

It should be noted that, owing to the 1:20 scale and the 1-g test condition, the stress level cannot fully replicate the prototype condition, leading to the potential differences in sand dilatancy and shear strength. Subsequent numerical simulations will be carried out to apply the tests data to the prototype engineering. And the results will be compared with the practical engineering data for correction. This study was conducted under monotonic loading conditions, whereas actual marine aquaculture foundations are typically subjected to cyclic loads. The results only provide a reference for the ultimate bearing capacity, motion behavior and strain at loading point of PVC suction caissons under monotonic loading, which can provide a reference for the behaviors of the suction caissons under cyclic loads and for practical engineering design.

REFERENCES

[1] FAO. The State of World Fisheries and Aquaculture 2026 [R]. Rome: Food and Agriculture Organization of the United Nations 2026.

[2] Wang CM, Ma M, Chu Y, *et al*. Developments in modeling techniques for reliability design of aquaculture cages: A review[J]. Journal of Marine Science and Engineering 2024; 12(1): 103. https://doi.org/10.3390/jmse12010103

[3] Yang YC, Liu HX, Sheng ZG. Applicability analyses on the end-bearing capacity of gravity installed anchors in clay[J], Ocean Engineering 2023; 283: 115101. https://doi.org/10.1016/j.oceaneng.2023.115101

[4] Wang Y, Liu P, Liu B, *et al*. Experimental Study on Bearing Characteristics of Pile-Anchor Foundations for Floating Offshore Wind Turbines Under Inclined Loading[J]. Journal of Marine Science and Engineering 2025; 13: 1890. https://doi.org/10.3390/jmse13101890

[5] James B, Edward L, Mohamed R, *et al*. The performance of shared suction caisson anchors in sand for floating offshore wind arrays with taut and catenary mooring[J]. Ocean Engineering 2026; 353(2): 124572. https://doi.org/10.1016/j.oceaneng.2026.124572

[6] Melchers RE. Long-Term Marine Corrosion Under the Influence of Microbiologically Influenced Corrosion and Calcareous Conditions[J]. Corros. Mater. Degrad 2025; 6: 46. https://doi.org/10.3390/cmd6040046

[7] Vinyl Sheet Piles: Corrosion-Free Solution for Marine Projects [EB/OL], 2026. https://www.easypiling.com/news/vinyl-sheet-piles-corrosionfree-solution-for-marine-projects.html

[8] Li D, He P, Zhang Y, Wu Y, *et al*. Model test on extraction behavior of suction caisson in layered soil under axial loading[J]. Marine Georesources & Geotechnology 2026; 1-21. https://doi.org/10.1080/1064119X.2026.2613334

[9] Houlsby GT, Byrne BW. Design procedures for installation of suction caissons in clay and other materials[J]. Proceedings of the Institution of Civil Engineers - Geotechnical Engineering 2005; 158(2): 75-82. https://doi.org/10.1680/geng.2005.158.2.75

[10] Houlsby GT, Byrne BW. Design procedures for installation of suction caissons in sand[J]. Proceedings of the Institution of Civil Engineers - Geotechnical Engineering 2005; 158(3): 135-144. https://doi.org/10.1680/geng.158.3.135.66297

[11] Liang H, Wu YQ, Li DY, *et al*. Inclined pull-out bearing capacity and failure mode of scaled suction caisson under different loading rates, Ocean Engineering 2026; 356(1): 125231. https://doi.org/10.1016/j.oceaneng.2026.125231

[12] Yang N, Zhou M, Tian Y, *et al*. Numerical investigation on the pullout capacity of suction caissons in silty sand-over-clay deposit[J]. Canadian Geotechnical Journal 2025; 62: 1-16. https://doi.org/10.1139/cgj-2023-0555

[13] Cheng L, Hossain MS, Hu Y, *et al*. Inclined loading of suction caisson anchors in calcareous sand with particle breakage[J]. Computers and Geotechnics 2024; 173: 106545. https://doi.org/10.1016/j.compgeo.2024.106545

[14] Bi QX. Cable tension formulation of deep-water gravity net cage group in current[D]. Shandong University 2023; (in Chinese) https://doi.org/10.27272/d.cnki.gshdu.2023.007895

[15] Bai Y, Li DY, *et al*. Failure modes and inclined bearing capacity of a modified suction caisson in sand[J]. Applied Ocean Research 2025; 155: 104416. https://doi.org/10.1016/j.apor.2025.104416

[16] Gupta PK, Verma VK. Study of concrete-filled unplasticized poly-vinyl chloride tubes in marine environment[J]. Proceedings of the Institution of Mechanical Engineers Part M Journal of Engineering for the Maritime Environment 2016; 230(2): 229-240. https://doi.org/10.1177/1475090214560448

[17] Gupta PK, Verma VK. Finite element modelling of load-carrying capacity of concrete-filled unplasticised polyvinyl chloride (UPVC) tubes exposed to marine environment. Ships and Offshore Structures[J] 2020; 16(3): 271-279. https://doi.org/10.1080/17445302.2020.1794556

[18] Zongping C, Ruitian X, Yuhan L, *et al*. Experimental study and finite element analysis on axial compression performance of CFRP-PVC confined coral seawater and sea-sand concrete columns[J]. Engineering Structures 2024; 302: 117443. https://doi.org/10.1016/j.engstruct.2024.117443

[19] Chen Z, Xu R. Experimental and numeral investigation on self-compacting concrete column with CFRP-PVC spiral reinforcement. Earthq Struct 2022; 22(1): 39-51. https://doi.org/10.12989/eas.2022.22.1.039

[20] Li JL. Wang LJ, Fan K, *et al*. Fatigue Analysis for Floating Wind Power Suction Anchor Structures [J]. Ship Engineering 2025; 47(S1): 58-63. (in Chinese) https://doi.org/10.13788/j.cnki.cbgc.2025.S1.011

[21] Davies GAO, Hitchings D, Zhou G. Impact Resistance of Marine Sandwich Composites[M]//Guedes Soares C, Santos T A. Maritime Technology and Engineering. London: Taylor & Francis Group 2015; 607-618. https://doi.org/10.13140/RG.2.1.4837.7044

[22] Gu SW. Study on Global Response and Mooring Optimization Design of Deep-water Gravity Cage System [D]. Harbin Engineering University 2024; (in Chinese) https://doi.org/10.27060/d.cnki.ghbcu.2024.000325

[23] Cerfontaine B, Collin F, Charlier R. Numerical modelling of transient cyclic vertical loading of suction caissons in sand[J]. Geotechnique 2016; 66(2): 121-136. https://doi.org/10.1680/jgeot.15.P.061

[24] Kelly RB, Houlsby GT, Byrne BW. Transient Vertical Loading of Model Suction Caissons in a Pressure Chamber. Geotechnique 2006; 56(10): 665-675. https://doi.org/10.1680/geot.2006.56.10.665

[25] Feng W, Fenglin H. Review and cost analysis of anchored foundation for floating offshore wind turbine [J]. Southern Energy Construction 2026; 1-13. https://doi.org/10.16516/j.ceec.2024-435

https://doi.org/10.65904/3083-3590.2026.02.08